Cenozoic benthic foraminiferal Mg/Ca and Li/Ca records: Toward unlocking temperatures and saturation states

Caroline H. Lear,[1] Elaine M. Mawbey,[1] and Yair Rosenthal[2]

[1] The sensitivities of benthic foraminiferal Mg/Ca and Li/Ca to bottom water temperature and carbonate saturation state have recently been assessed. Here we present a new approach that uses paired Mg/Ca and Li/Ca records to calculate simultaneous changes in temperature and saturation state. Using previously published records, we first use this approach to document a cooling of deep ocean waters associated with the establishment of the Antarctic ice sheet at the Eocene-Oligocene climate transition. We then apply this approach to new records of the Middle Miocene Climate Transition from ODP Site 761 to estimate variations in bottom water temperature and the oxygen isotopic composition of seawater. We estimate that the oxygen isotopic composition of seawater varied by ~1‰ between the deglacial extreme of the Miocene Climatic Optimum and the glacial maximum following the Middle Miocene Climate Transition, indicating large amplitude variations in ice volume. However, the longer-term change between 15.3 and 12.5 Ma is marked by a ~1°C cooling of deep waters, and an increase in the oxygen isotopic composition of seawater of ~0.6‰. We find that bottom water saturation state increased in the lead up to the Middle Miocene Climate Transition and decreased shortly after. This supports decreasing pCO_2 as a driver for global cooling and ice sheet expansion, in agreement with existing boron isotope and leaf stomatal index CO_2 records but in contrast to the published alkenone CO_2 records.

Citation: Lear, C. H., E. M. Mawbey, and Y. Rosenthal (2010), Cenozoic benthic foraminiferal Mg/Ca and Li/Ca records: Toward unlocking temperatures and saturation states, *Paleoceanography*, *25*, PA4215, doi:10.1029/2009PA001880.

1. Introduction

[2] Earth's transition from the warm, ice-free climate of the early Cenozoic to today's icehouse world is recorded by an overall ~4‰ increase in the benthic foraminiferal oxygen isotope ($\delta^{18}O$) record over the past ~50 million years [*Shackleton and Kennett*, 1975; *Miller et al.*, 1987; *Zachos et al.*, 2001]. This benthic $\delta^{18}O$ record reflects both a ~12°C cooling and the growth of Earth's cryosphere to its present size and isotopic composition. Earth's cryospheric development was not a smooth process during this time; for example major glaciation "events" are recorded by relatively rapid shifts in the oxygen isotope records on the order of ~1‰ in the earliest Oligocene and middle Miocene. The driving mechanism for the expansion of the Antarctic ice sheet during the Middle Miocene Climate Transition (MMCT) is not known, although increased burial rates of organic carbon leading to atmospheric CO_2 drawdown has been proposed [*Vincent and Berger*, 1985; *Flower and Kennett*, 1993]. A detailed pCO_2 record based on the $\delta^{13}C$ composition of alkenones displays little variation, thus apparently implying a decoupling of pCO_2 and Neogene climate [*Pagani et al.*,

1999, 2009]. In contrast, evidence from boron isotope ratios in planktonic foraminifera and a leaf stomatal index record both suggest a ~150 ppmV CO_2 decrease in the middle Miocene (possibly transient), which might explain the MMCT glaciation [*Pearson and Palmer*, 2000; *Kürschner et al.*, 2008]. Resolving the cause of this glaciation therefore has important bearing on our understanding of the role of CO_2 in the evolution of Earth's climate.

[3] The implications of the two above scenarios for the ocean carbonate chemistry should have been substantially different. The relatively constant atmospheric pCO_2, suggested from the alkenone records implies a relatively constant total carbon (TCO_2) to total alkalinity (Talk) ratio with the corollary of a relatively constant lysocline and calcite compensation depth (CCD). In contrast, the changes in atmospheric pCO_2 suggested from the boron isotope and stomatal index records should reflect changes in the TCO_2/Talk ratio between deep and surface waters, implying changes in the carbonate saturation of the deep ocean and therefore the depth of the lysocline. Here we propose a new method for reconstructing changes in the calcite saturation level of the deep ocean and apply it to the Middle Miocene Climate Transition.

[4] The salinity-independent benthic foraminiferal Mg/Ca paleothermometer has been shown to have potential in deconvolving bottom water temperature (BWT) and ice volume from the $\delta^{18}O$ record [*Lear et al.*, 2000; *Martin et al.*, 2002; *Billups and Schrag*, 2002; *Lear et al.*, 2004; *Shevenell et al.*, 2008; *Sosdian and Rosenthal*, 2009]. Benthic foraminiferal Mg/Ca records from deep-sea sites

[1]School of Earth and Ocean Sciences, Cardiff University, Cardiff, UK.

[2]Institute of Marine and Coastal Sciences and Department of Geological Sciences, Rutgers, State University of New Jersey, New Brunswick, New Jersey, USA.

across the glaciation event in the earliest Oligocene have failed, however, to document a cooling signal [*Lear et al.*, 2000; *Billups and Schrag*, 2003; *Lear et al.*, 2004]. With no apparent cooling, the shift in the benthic $\delta^{18}O$ record implies substantial bipolar glaciation, which is at odds with current model simulations of early Cenozoic climate under elevated atmospheric pCO_2 [*DeConto et al.*, 2008]. Alternatively, the Mg/Ca data might have been compromised by non-temperature-related effects. Modern benthic foraminifera living in poorly saturated waters have lower Mg/Ca than expected from global temperature calibrations. This discrepancy has been attributed to a saturation state control operating at low levels of saturation [*Martin et al.*, 2002; *Elderfield et al.*, 2006; *Yu and Elderfield*, 2008]. Indeed, recent work has quantified the sensitivity of benthic foraminiferal Mg/Ca to seawater saturation state [*Rosenthal et al.*, 2006; *Elderfield et al.*, 2006; *Yu and Elderfield*, 2008]. Therefore, an alternative interpretation of the early Oligocene Mg/Ca records is that they also reflect the increase in bottom water saturation state associated with the concomitant 1.2 km deepening of the calcite compensation depth (CCD) [*Coxall et al.*, 2005; *Lear et al.*, 2004]. In support of this, Mg/Ca temperature records of the earliest Oligocene glaciation from two shallow water (shelf-slope) sites display a ~2–3°C cooling, with inferred ice volume changes in line with independent estimates derived from sequence stratigraphy [*Lear et al.*, 2008; *Katz et al.*, 2008]. A global biogeochemical box model indicates that the early Oligocene CCD deepening was caused by the sea level fall via increased weathering of exposed shelf carbonates and decreased deposition of shelf carbonates [*Merico et al.*, 2008]. Therefore, it may be expected that other major glaciations of the Cenozoic are also associated with increases in bottom water saturation state.

[5] Benthic foraminiferal Li/Ca has also been shown to reflect changes in both seawater saturation state and temperature [*Hall and Chan*, 2004; *Marriott et al.*, 2004; *Lear and Rosenthal*, 2006]. Therefore, paired Mg/Ca and Li/Ca records may potentially be used simultaneously to reconstruct both temperature and saturation state from deep-sea records. Here, we test this novel approach on previous records of the earliest Oligocene glaciation, and then apply it to new records of the MMCT. Our seawater saturation state reconstruction records an increase in the lead up to the MMCT, supporting decreasing atmospheric CO_2 as the primary driving mechanism for global cooling and ice sheet expansion.

2. Materials and Methods

2.1. Miocene Samples From ODP Site 761

[6] Ocean Drilling Program (ODP) Site 761 is situated at 2179 m water depth on the Wombat Plateau, off northwest Australia (16°44.23′S, 115°32.10′E). Slow sedimentation rates have led to unusually shallow burial depths (<50 m) for the middle Miocene sequence, leading to enhanced foraminiferal preservation (Figure 1). 20 cc samples were taken at approximately 10 cm resolution. For an age model we use a fourth order polynomial fit through the biostratigraphic and isotopic datums provided by *Holbourn et al.* [2004]. Between

3 and 23 individuals of the benthic foraminifera *Oridorsalis umbonatus* were picked from the 250–355 μm size fraction and crushed between glass plates to open all chambers. Test fragments were cleaned using a protocol to remove clays, metal oxides and organic matter [*Boyle and Keigwin*, 1985]. Between the clay removal and reductive steps the samples were examined under a binocular microscope, and non-carbonate particles were removed using a fine paintbrush. Samples were dissolved in trace metal pure 0.065M HNO_3 and diluted with trace metal pure 0.5M HNO_3 to a final volume of 350 μl. Samples were analyzed at Cardiff University on a Thermo Element XR ICP-MS against standards with matched calcium concentration to reduce matrix effects [*Lear et al.*, 2002]. Samples with a Li intensity signal less than five times greater than the analytical blank were discarded. All data for a sample were rejected when Al/Ca exceeded 150 μmol/mol and/or Fe/Ca exceeded 100 μmol/mol. Long-term precision as determined by analyzing an independent consistency standard during each run is ~1% and ~2% (r.s.d.) for Mg/Ca and Li/Ca, respectively. Although an isotope stratigraphy already exists for Site 761B [*Holbourn et al.*, 2004], we generated our own stratigraphy so that our trace metal records could be compared to isotope records from exactly the same interval. Approximately 8 individuals of *Cibicidoides mundulus* (250–355 μm) were crushed, ultrasonicated in methanol to remove clays and oxidized with 3% H_2O_2 to remove organic matter. Approximately half of each sample was analyzed on a ThermoFinnigan MAT252 with online sample preparation using an automated Kiel III carbonate device. Results are reported relative to PDB, and long-term uncertainty based on repeat analysis of NBS-19 is ± 0.08‰ (2σ).

2.2. Mg/Ca Temperature Sensitivity

[7] A global compilation of the benthic foraminiferal genus *Cibicidoides* suggested Mg/Ca temperature sensitivity to be on the order of 10% per °C, in line with sensitivities determined for planktonic foraminifera [*Lear et al.*, 2002]. A core top calibration for *Oridorsalis umbonatus* in the same study produced a similar albeit slightly higher sensitivity [*Lear et al.*, 2002]. These global compilations include samples from highly saturated waters on the Little Bahama Banks, and it has been suggested that a diagenetic contribution of high-Mg calcite to these samples caused the calibration curve to be artificially steepened [*Marchitto et al.*, 2007; *Curry and Marchitto*, 2008]. A lower and linear Mg/Ca temperature sensitivity based on *C. pachyderma* from the Florida Straits of 0.12 mmol/mol per °C has therefore been proposed [*Marchitto et al.*, 2007]. In core top samples where the two species *C. pachyderma* and *O. umbonatus* occur we find that *O. umbonatus* Mg/Ca is 0.2 ± 0.02 greater than *C. pachyderma*. Therefore we subtract 0.2 mmol/mol from new and published *O. umbonatus* core top data [*Lear et al.*, 2002] (auxiliary material) to compare to the published *C. pachyderma* temperature calibration (Figure 2).[1] We use sites with bottom water saturation states ranging between 7 and 62 μmol/kg, and find that combining the *C. pachyderma* and *O. umbonatus*

[1]Auxiliary materials are available at ftp://ftp.agu.org/apend/pa/2009pa001880.
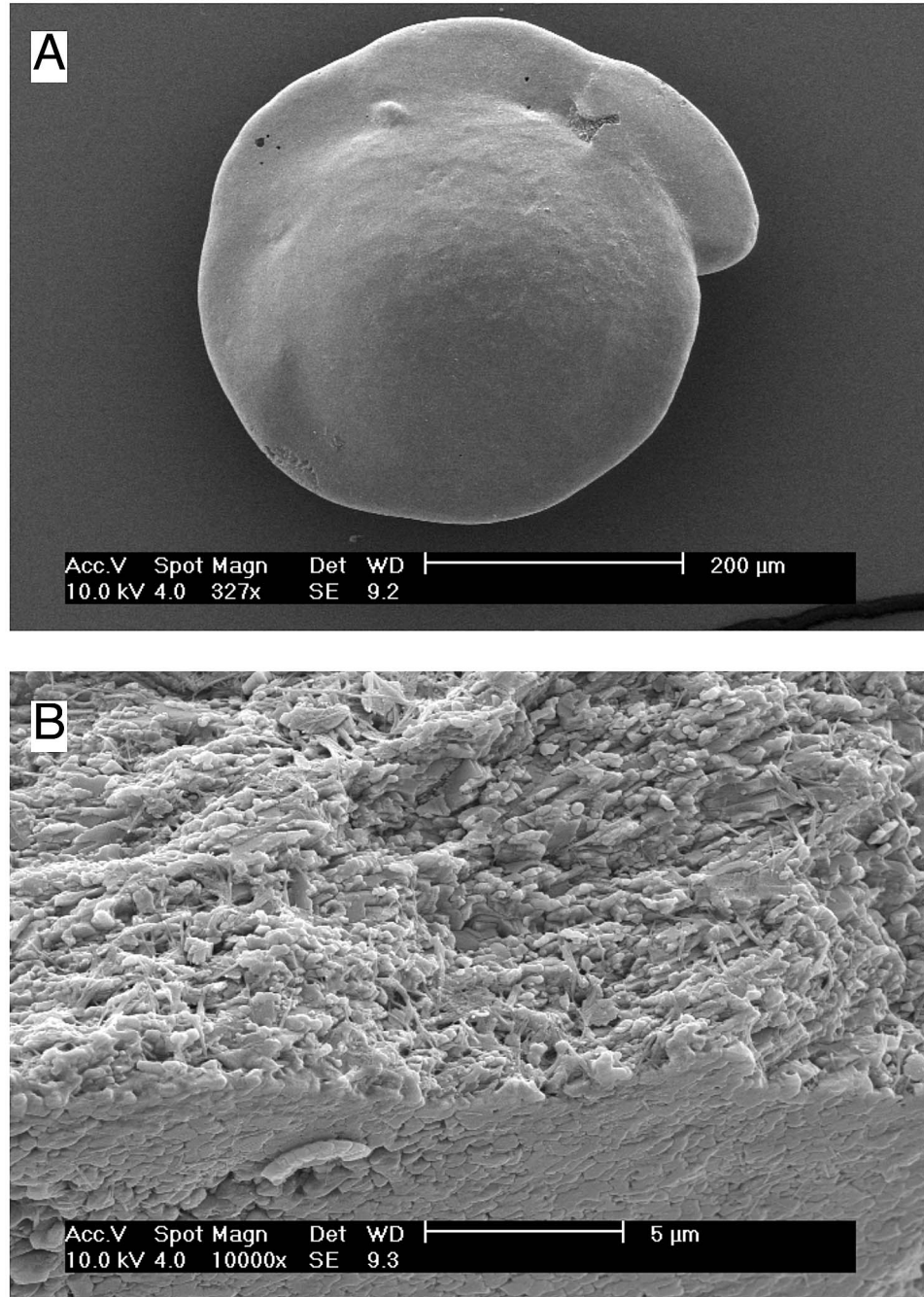
Figure 1. (a) Whole test of *Oridorsalis umbonatus*, from ODP 761B 05-03 8–10 cm (35.78 m below seafloor). (b) Cross section through test wall of *O. umbonatus* from ODP 761B 05-07 38–40 cm (42.08 m below seafloor) displaying original microstructure.

Mg/Ca data in this way does not change the intercept or slope of the original calibration equation (Figure 2a). Note that the same intercept and slope are obtained if we use only sites where the bottom water saturation state is greater than 25 μmol/kg (above the proposed threshold for saturation state effects on Mg/Ca [*Yu and Elderfield*, 2008]). This suggests that the 0.12 mmol/mol per °C sensitivity of *Marchitto et al.* [2007] may be applied to *O. umbonatus* Mg/Ca records

(Figure 2). Based on the core top calibration data, the error (1 s.e.) on the Mg/Ca temperature sensitivity is 2.1°C.

2.3. Mg/Ca Saturation State Sensitivity

[8] *Elderfield et al.* [2006] quantify the saturation state effect on benthic foraminiferal Mg/Ca by using the temperature sensitivity obtained in warm waters to subtract the temperature effect from cold (<3°C), deep water samples
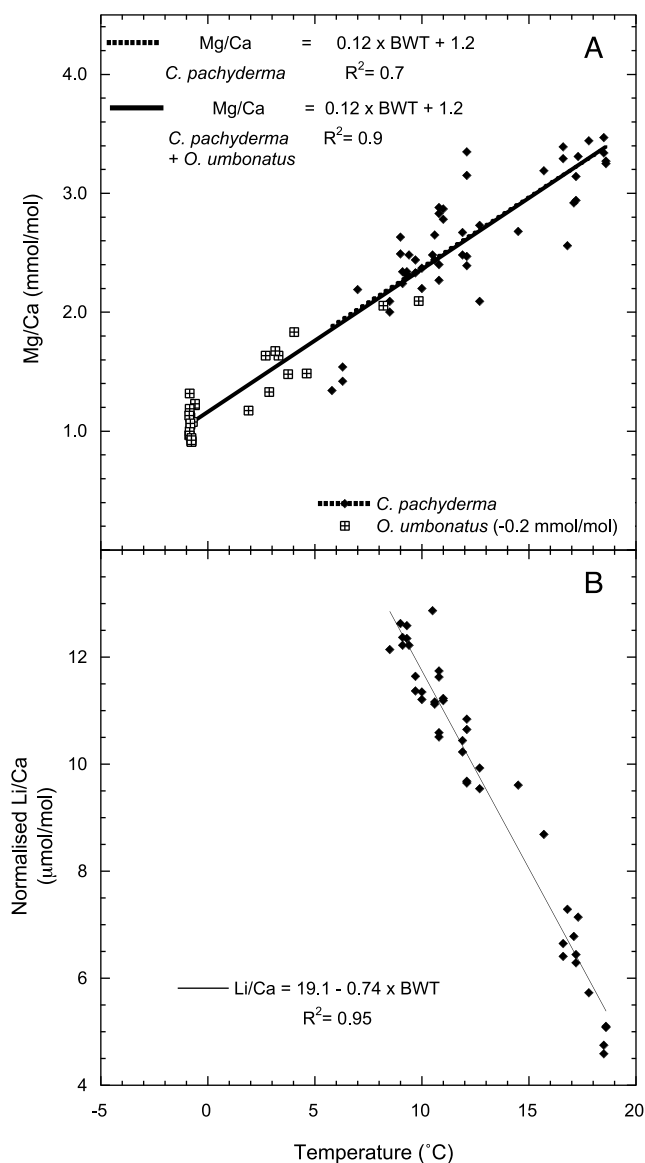
Figure 2. Compiled published and new core top data from saturated waters used to estimate the temperature sensitivities for benthic foraminiferal Mg/Ca and Li/Ca (see text for details). (a) *C. pachyderma* Mg/Ca [*Bryan and Marchitto*, 2008] and *O. umbonatus* Mg/Ca [*Lear et al.*, 2002] (new data presented in auxiliary material). *O. umbonatus* Mg/Ca ratios have been corrected by −0.2 mmol/mol to account for an interspecies offset from *C. pachyderma*. The combined data set has an identical slope and intercept to the original regression based solely on *C. pachyderma* [*Bryan and Marchitto*, 2008]. (b) *C. pachyderma* Li/Ca [*Bryan and Marchitto*, 2008] normalized to a common saturation state of 50 μmol/kg using the Li/Ca saturation state sensitivity of 0.046 μmol/mol/μmol/kg determined on *O. umbonatus* (see text for details).

where both temperature and saturation state typically covary. Using the temperature sensitivity described in section 2.2 yielded a sensitivity of 0.0086 ± 0.0006 mmol/mol/μmol/kg for *Cibicidoides wuellerstorfi* [*Elderfield et al.*, 2006]. This estimate is in excellent agreement with a later study by *Yu and Elderfield* [2008]. There is likely a threshold above which the saturation state effect on benthic foraminiferal Mg/Ca ratios is negligible, and it has been suggested that this may be ~25 μmol/kg [*Yu and Elderfield*, 2008; *Healey et al.*, 2008]. Our *O. umbonatus* core top data from the Norwegian Sea and New Zealand suggest a similar sensitivity and shall be discussed in detail elsewhere. Therefore, for this study we use a sensitivity of benthic foraminiferal Mg/Ca to changing saturation state of 0.0086 mmol/mol/μmol/kg. Based on the core top calibration data, the error (1 s.e.) on the Mg/Ca saturation state sensitivity is 13 μmol/kg. Future work should be aimed at better constraining this sensitivity for different species of benthic foraminifera.

2.4. Li/Ca Saturation State Sensitivity

[9] Downcore benthic and planktonic Li/Ca records display a relatively large (13–40%) decrease across the last Pleistocene deglaciation, which cannot be attributed to temperature [*Burton and Vance*, 2000; *Hall and Chan*, 2004]. *Hall and Chan* [2004] hypothesized that the Li/Ca decrease reflects lower calcification rate caused by decreased seawater carbonate ion concentration on the transition from the last glacial maximum to the Holocene. Core top data from a holothermal water depth transect in the Norwegian Sea suggested that the sensitivity of benthic foraminiferal (*O. umbonatus*) Li/Ca to carbonate saturation state is 0.052 μmol/mol/μmol/kg [*Lear and Rosenthal*, 2006]. *Lear and Rosenthal* [2006] did not correct for the addition of anthropogenic carbon to the water column as some of the benthic foraminifera were apparently alive at the time of collection. However, to be consistent with other workers [*Yu and Elderfield*, 2008] and acknowledging the greater abundance of dead specimens in the samples, we now correct the water column data for the input of anthropogenic carbon [*Sabine et al.*, 2004]. This has had the effect of changing the Li/Ca saturation state sensitivity from 0.052 to 0.047 μmol/mol/μmol/kg. Based on the core top calibration data, the error (1 s.e.) on the Li/Ca saturation state sensitivity is 13 μmol/kg. Unlike benthic foraminiferal Mg/Ca, core top data suggest a linear relationship between benthic foraminiferal Li/Ca and bottom water saturation state that extends into well-saturated waters with no apparent threshold.

2.5. Li/Ca Temperature Sensitivity

[10] Core top samples of *Uvigerina sp.* from the Arabian Sea display an overall increase in Li/Ca with increasing water depth, which has been interpreted as suggesting a negative Li/Ca temperature sensitivity of 2.5% per °C [*Marriott et al.*, 2004]. However, these core top data may also be affected by a saturation state control on Li/Ca, which would mean that the 2.5% sensitivity is an underestimate. As our core top *O. umbonatus* Li/Ca data span a very limited temperature range at the cold end of the calibration we rely here on the calibration of *Bryan and Marchitto* [2008], which is based

on a depth transect from the Florida Straits. We estimate the Li/Ca temperature sensitivity by subtracting the ΔCO_3^{2-} effect on their Li/Ca data. To do this we first recalculated the saturation states given in the Florida Straits data set to subtract the effect of the input of anthropogenic carbon, as the foraminifera analyzed were not living during the time of collection [*Sabine et al.*, 2004; *Bryan and Marchitto*, 2008]. Our recalculated saturation states are provided in the auxiliary material. We then used our Li/Ca saturation state sensitivity based on *O. umbonatus* (section 2.4) to normalize the *C. pachyderma* Li/Ca data to a common saturation state of +50 μmol/kg (see auxiliary material). This preliminary approach to determining the sensitivity of benthic foraminiferal Li/Ca to temperature reveals a remarkably good linear fit for warmer temperatures but suggests a smaller sensitivity to temperature below 5°C. It is unlikely that Middle Miocene temperatures at our Site cooled below 5°C, so we calculate the linear regression between the normalized Li/Ca data and temperature for temperatures greater than 8°C. This approach yielded a Li/Ca temperature sensitivity of −0.74 μmol/mol/°C with a good correlation coefficient (r^2 = 0.95) (Figure 2). Based on these core top calibration data, the error (1 s.e.) on the Li/Ca temperature sensitivity is 0.75°C. We acknowledge the combination of two different foraminiferal species in calculating this sensitivity, and note that future work should be aimed at better constraining this sensitivity for different species of benthic foraminifera. In addition, further work should especially focus on the "cold end" of the calibration, where the sensitivity may be lower, to enable application to younger/colder time intervals.

2.6. Calculating Temperature and Saturation State Variations Below the Mg/Ca Saturation State Threshold

[11] We use the sensitivities described above and assume that temporal variations in Mg/Ca (ΔMg) and Li/Ca (ΔLi) solely reflect a unique combination of temporal variations in temperature and saturation state change.

[12] Therefore, for intervals where Mg/Ca is affected by a saturation state effect:

$$\Delta Mg = 0.0086.\Delta CO_3^{2-} + 0.12.\Delta T \qquad (1)$$

$$\Delta Li = 0.047.\Delta CO_3^{2-} - 0.74.\Delta T \qquad (2)$$

hence

$$\Delta T = (\Delta Mg - 0.183.\Delta Li)/0.225 \qquad (3)$$

$$\Delta CO_3^{2-} = (\Delta Mg + 0.162.\Delta Li)/0.0162 \qquad (4)$$

Based on core top calibration data, the errors (1 s.e.) on the Mg/Ca sensitivities presented above are 2.1°C and 13 μmol/kg for temperature and saturation state, respectively, and the errors (1 s.e.) on the Li/Ca sensitivities presented above are 0.75°C and 13 μmol/kg for temperature and saturation state, respectively. The errors for temperature and saturation state in our pooled equations (equations (3) and (4)) are therefore 2.2°C and 18.4 μmol/kg. For our Middle Miocene down core record, we apply the calibrations to smoothed data (5 point

moving average), and hence the corresponding standard errors for the smoothed record are smaller i.e., 1.1°C and 9 μmol/kg.

[13] By assuming a value for the temperature and saturation state (ΔCO_3^{2-}) of our oldest sample we can therefore calculate both temperature and saturation state through the MMCT. We use the *Marchitto et al.*, 2007 calibration (after a correction of −0.2 mmol/mol is applied to account for the interspecies offset between *O. umbonatus* and *C. pachyderma*) to estimate the temperature of the oldest sample. For simplicity we use modern seawater Mg/Ca values, as we believe this method is more robust in determining relative temperature changes rather than absolute temperature changes, but note that if we assumed lower seawater values for the middle Miocene, then our calculated absolute temperatures would be somewhat higher. We use a value of 0 μmol/kg for the initial saturation state of the record (at 16.97 Ma, not shown) and stress that we are estimating relative variations in bottom water saturation state only. We note that a temperature calibration based on benthic foraminiferal Mg/Li ratios has recently been proposed, which gives similar results as the equations set out here [*Bryan and Marchitto*, 2008]. However, we prefer our approach, as the sensitivities of Mg/Ca and Li/Ca to both temperature and saturation state have been determined independently, and thus it should be more accurate for situations when variations in both trace metal records are dominated solely by temperature. To calculate $\delta^{18}O$ of seawater we use the benthic equation of *Shackleton* [1974] after applying a +0.5‰ equilibrium offset for *Cibicidoides*:

$$\text{Temperature} = 16.9 - 4.0(\delta^{18}O_{FORAM} - \delta^{18}O_{SW}) \qquad (5)$$

2.7. Application of Method to Existing Records of the Eocene-Oligocene Climate Transition

[14] Here we discuss previously published Eocene-Oligocene trace metal data from Deep Sea Drilling Project (DSDP) Site 522 (26°6.843′S, 5°7.784′W; 4441 m below sea level (mbsl)) and ODP Site 1218 (8°53.378′N, 135° 22.00′W; 4828 mbsl). Benthic foraminiferal Li/Ca increases from 11.3 to 13.2 μmol/mol across the Eocene-Oligocene climate transition at ODP Site 1218 [*Lear and Rosenthal*, 2006]. Benthic foraminiferal Mg/Ca increases by 0.28 mmol/mol at Site 1218 and shows no overall change at DSDP Site 522 [*Lear et al.*, 2000, 2004]. Benthic foraminifera from DSDP Site 522 have not been analyzed for Li/Ca, so for the purpose of this discussion we assume the 1.9 μmol/mol increase observed at ODP Site 1218 is also representative of DSDP Site 522. This assumption may not be entirely valid as the Atlantic CCD may have deepened to a somewhat smaller extent than the Pacific CCD at this time [*Hsü et al.*, 1984; *Rea and Lyle*, 2005]. Nevertheless, we consider this a useful exercise in testing the first order applicability of the method. Using equation 3 implies that deep ocean temperatures cooled by ~1.5°C at DSDP Site 522 and by 0.3°C at ODP Site 1218, whereas bottom water saturation state increased by 19 μmol/kg at Site 522 and by 36 μmol/kg at Site 1218. To put these values into context, a ~2.5°C tropical sea surface cooling has recently been documented from Tanzanian sediments, and the 1.2 km CCD deepening could be accounted for by an increase
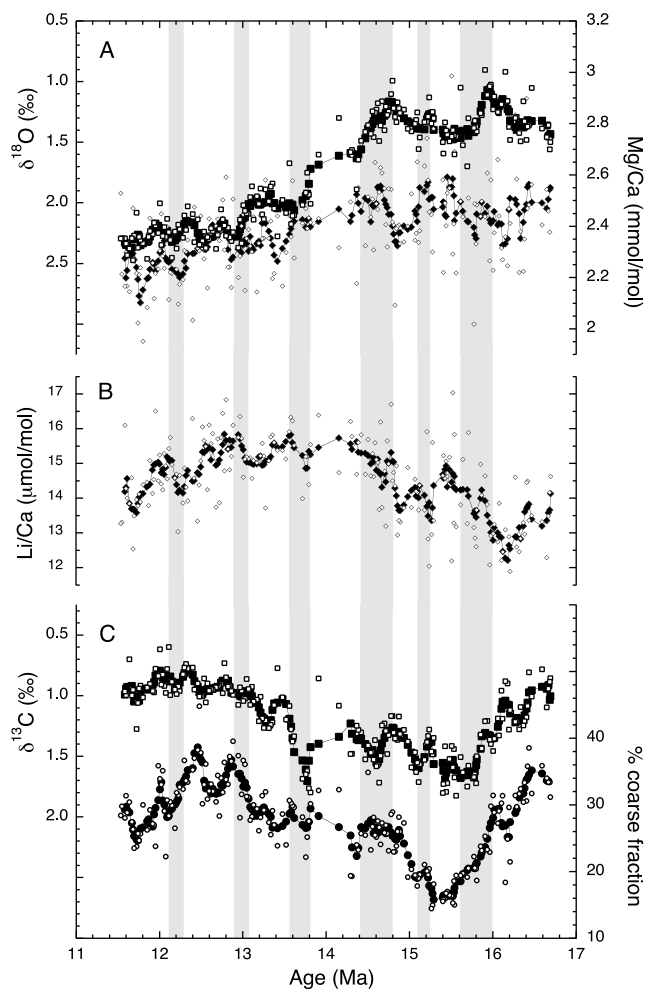
Figure 3. Stable isotope, trace metal, and % coarse fraction data from ODP Site 761. (a) Benthic foraminiferal (*C. mundulus*) oxygen isotopes (raw data as open squares, 5-point moving average as closed squares) and benthic foraminiferal (*O. umbonatus*) Mg/Ca (raw data as open diamonds, 5-point moving average as closed diamonds). (b) Benthic foraminiferal (*O. umbonatus*) Li/Ca (raw data as open diamonds, 5-point moving average as closed diamonds). (c) Benthic foraminiferal *(C. mundulus)* carbon isotopes (raw data as open squares, 5-point moving average as closed squares) and the % coarse fraction of the sediment (proportion greater than 63 μm diameter) (raw data as open circles, 5-point moving average as closed circles). Vertical bars highlight stepped increases in the oxygen isotope record, which correspond to increases in the benthic foraminiferal Li/Ca record.

in bottom water (CO_3^{2-}) of 19 μmol/kg [*Broecker and Peng*, 1982; *Lear et al.*, 2008]. This revised estimate for the temperature history at DSDP Ste 522 cannot be rigorously evaluated as a Li/Ca record for DSDP Site 522 may be different from ODP Site 1218, yet it seems an improvement over the previous interpretation of no temperature change [*Lear et al.*, 2000]. However, the revised temperature estimate for ODP Site 1218 cannot be reconciled with our current understand-

ing of the climate transition [*Lear et al.*, 2008; *DeConto et al.*, 2008]. We interpret this discrepancy as reflecting a dissolution effect on benthic foraminiferal Mg/Ca in the undersaturated waters at ODP Site 1218 (paleowater depth ~3.7 km) prior to the climate transition [*Mawbey et al.*, 2009]. ODP Site 1218 is unusual in that it was situated close to the CCD immediately prior to the 1.2 km CCD deepening across the Eocene-Oligocene climate transition, with the result that benthic foraminifera are noticeably dissolved and planktonic foraminifera are scarce or more commonly absent. Quantifying such a dissolution effect is not trivial, as it is rare to find significant numbers of modern calcite foraminifera preserved in undersaturated waters, although preliminary core top data from severely undersaturated waters also suggest a dissolution effect on benthic foraminiferal Mg/Ca [*Jordan*, 2008]. By extension, this proposed dissolution effect is not likely to be applicable to the vast majority of paleoceanographic records, due to the scarcity of foraminifera in such sediments. While it is still not a straightforward matter to unravel the complex climatic and chemical changes across the Eocene-Oligocene transition, the new approach presented here demonstrates the potential use of combined Li/Ca and Mg/Ca paleothermometry to reconstruct bottom water temperatures even when there have been significant changes in bottom water saturation state.

3. Results

[15] Our benthic foraminiferal oxygen isotope stratigraphy for ODP Site 761B is in excellent agreement with that published earlier by *Holbourn et al.* [2004]. All new data presented in this paper are available as auxiliary material. As we determine temperatures and saturation states using an iterative approach based on simultaneous changes in Mg/Ca and Li/Ca throughout the record, we use a 5-point moving average of benthic foraminiferal $\delta^{18}O$, Mg/Ca and Li/Ca (Figure 3). In constructing these records we only used samples where we produced reliable data for all three variables (see section 2). Benthic foraminiferal Mg/Ca decreases across the MMCT, from around 2.5 mmol/mol to around 2.2 mmol/mol (Figure 3). Li/Ca displays an overall increasing trend (from ~12 μmol/mol to ~15.5 μmol/mol) between 16 Ma and 13.5 Ma, and a subsequent decreasing trend (from ~15.5 μmol/mol to ~14 μmol/mol) between 13.5 and 11.5 Ma (Figure 3). Superimposed on this general trend are what appear to be cyclical variations in Mg/Ca and Li/Ca. Benthic Mg/Ca fluctuates with an amplitude between 0.1 and 0.2 mmol/mol (Figure 3). Similarly, the benthic foraminiferal Li/Ca record displays relatively rapid (<100 kyr) increases that appear to be contemporaneous with the rapid increases in the oxygen isotope record, at ~15.8 Ma, 15.2 Ma, 14.6 Ma, 13.7 Ma, 13.0 Ma and 12.2 Ma (Figure 3). We also present benthic foraminiferal $\delta^{13}C$ and sediment % coarse fraction (>63 μm) (Figure 3). These two records show some similarities in their general trends. Benthic foraminiferal $\delta^{13}C$ generally becomes lighter through the climate transition, between ~15 Ma and 12 Ma. Over the same time interval the sediment % coarse fraction generally increases. Although there are shorter-term variations within the $\delta^{13}C$ and sediment

% coarse fraction records, there is no consistent relationship between these and the steps within the $\delta^{18}O$ record.

4. Discussion: Middle Miocene Climate Transition

[16] Our new trace metal and stable isotope records span a ~5 m.y. interval from the warmth of the Miocene Climatic Optimum through the Middle Miocene Climate Transition. It is possible that these long-term trace metal records may reflect changes in the seawater concentrations of magnesium, lithium and calcium in addition to changes in temperature and carbonate saturation state. The residence time of magnesium is long relative to the length of our record (~10 m.y. [*Broecker*

and Peng, 1982]), but the residence times of lithium and calcium are shorter (~3 m.y. and ~1 m.y., respectively [*Stoffynegli and MacKenzie*, 1984; *Broecker and Peng*, 1982]). Therefore, changes in seawater (Ca) in particular have a potential to affect our interpretations. However, we note that if our records were dominated by changes in seawater (Ca) we would expect to see similar trends in the Mg/Ca and Li/Ca records, which is not observed (Figure 3). Because no high-resolution estimates of the variation of these seawater concentrations exist, we assume they are constant over the interval studied for the purpose of the discussion below. While we acknowledge that this assumption may limit the accuracy of our long-term temperature and saturation state reconstructions we note that most of the cooling of the MMCT occurs in a few relatively rapid "steps" between 14.7 and 12.7 Ma. It is unlikely that seawater (Mg), (Ca) or (Li) changed significantly on these short (~100 kyr) time scales, suggesting that our interpretation of temperature and saturation state changes across these steps are relatively robust.

4.1. Middle Miocene Temperatures and Ice Volumes

[17] ODP Site 761 is currently situated at 2179 m water depth, with a bottom water saturation state around 30 μmol/kg. This level may be close to the threshold for a saturation state effect on benthic foraminiferal Mg/Ca (see section 2.2). Therefore we take two approaches in calculating bottom water temperatures from our *Oridorsalis umbonatus* Mg/Ca record. The first is to assume that 100% of the variability in the Mg/Ca record reflects temperature variations, and we use the equation of *Marchitto et al.* [2007] to calculate BWT after subtracting 0.2 mmol/mol to account for an interspecies offset between *O. umbonatus* and *C. pachyderma* and using modern seawater Mg/Ca values. These are the "uncorrected temperatures" shown in Figure 4a. Our second approach in calculating BWT is to assume that changes in saturation state at this site in the middle Miocene did impact the Mg/Ca record,
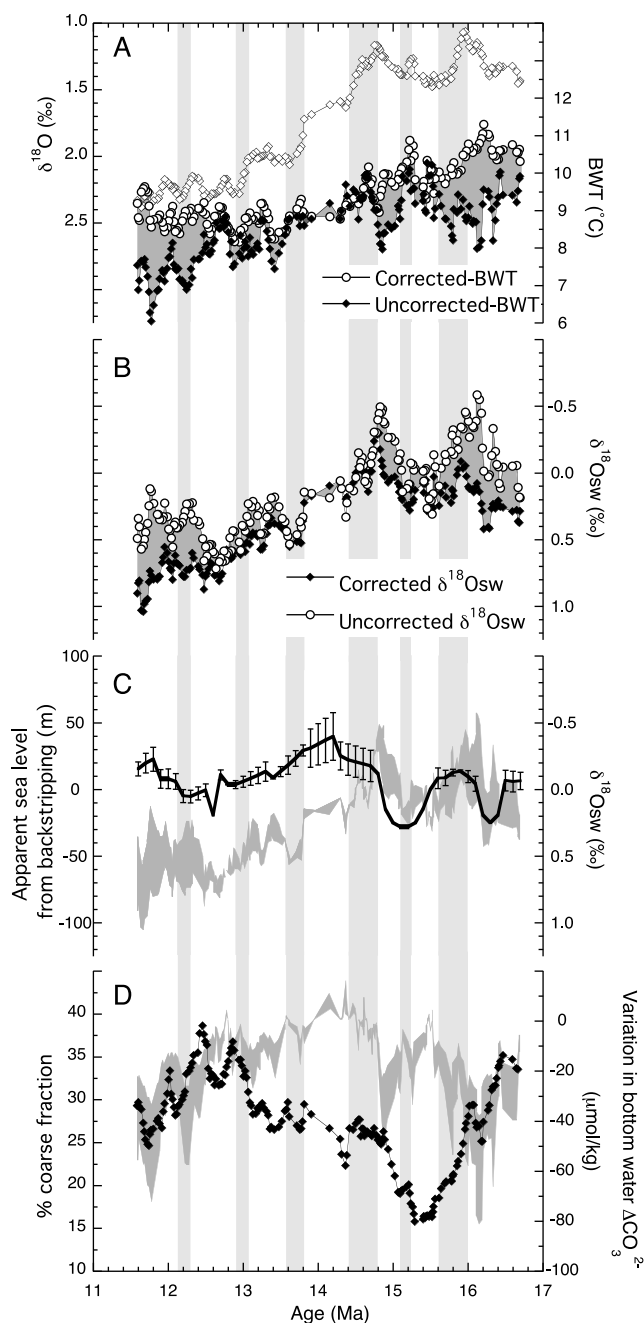
Figure 4. (a) Five-point moving average data for benthic foraminiferal (*C. mundulus*) oxygen isotopes (open diamonds) and uncorrected (open circles) and corrected (closed diamonds) bottom water temperatures based on the data shown in Figure 3 (see text for details). (b) Seawater $\delta^{18}O$ (‰ versus PDB) calculated using the $\delta^{18}O$ data and the uncorrected (open circles) and corrected (closed diamonds) temperatures shown in Figure 4a (see text for details). (c) Eustatic sea level estimates derived from backstripping New Jersey and Delaware core holes [*Kominz et al.*, 2008] multiplied by 1.48 to achieve "Apparent Sea Level" as detailed by *Pekar et al.* [2002] and the range of seawater $\delta^{18}O$ variation calculated in Figure 4b. Error bars on the sea level estimates are based on uncertainties related to original paleowater depth estimation within the backstripping method; the three portions of the curve with no error bars represent lowstands with correspondingly no material present in the shelf margin core holes [*Kominz et al.*, 2008]. (d) Five-point moving average data for the % coarse fraction of the sediment (proportion greater than 63 μm diameter) and range of calculated bottom water saturation state calculated using corrected and uncorrected temperatures (see text for details).

and we use equation 3 to calculate variations in bottom water temperature (section 2.6). These are the "corrected temperatures" in Figure 4a.

[18] Both the uncorrected Mg/Ca paleotemperature record and the saturation state–corrected paleotemperature record display an overall cooling of ~2°C across our record, between 16.7 and 12 Ma (Figure 4). This is in good agreement with previous estimates [*Lear et al.*, 2000; *Billups and Schrag*, 2002; *Shevenell et al.*, 2008]. When the original Mg/Ca and Li/Ca records vary in antiphase, most of the variance is attributed to temperature, and the difference between the corrected and uncorrected temperature records is small (e.g., across the MMCT, between ~13–15 Ma) (Figure 4). However, when the Li/Ca and Mg/Ca records vary in phase, much of the variance is ascribed to changing saturation state, so that the difference between the BWT records is larger (e.g., on the order of ~2°C around 16 Ma in the Miocene Climatic Optimum [*Flower and Kennett*, 1994]). The large range in calculated temperatures at this time therefore results from the uncertainty of the threshold at which our Mg/Ca record is affected by changes in saturation state. The Li/Ca record increases between 16 Ma and 13 Ma, which may reflect an increase in saturation state. Therefore it is possible that the Mg/Ca ratios have been affected by changes in saturation state in the oldest part of the record but not the younger part of the record. If so, the calculated temperatures would follow the trend of the corrected temperatures in the early portion of the record, and the trend of the uncorrected temperatures in the later portion of the record. Interestingly, we note that such a record would bear a striking resemblance to the benthic oxygen isotope record (Figure 4a). Nevertheless as we have no means at present to constrain the threshold at which the Mg/Ca record is affected by saturation state, we prefer to use a conservative approach and propose that the variation of BWT lies somewhere between our two reconstructed curves (shaded area in Figure 4a), while the error associated with each curve is around ±1°C (section 2.6).

[19] We use the range in temperature between our two curves (Figure 4a) in combination with our benthic oxygen isotope record (measured on *C. mundulus* from the same sediment samples) to calculate the seawater oxygen isotope ratio through the MMCT (Figures 4b and 4c). Our δ^{18}Osw record demonstrates that global ice volume increased across the MMCT, in agreement with the record of eustasy obtained using backstripping techniques on the Marion Plateau [*John et al.*, 2004]. A more recent study using backstripping techniques on New Jersey and Delaware core holes provides a higher resolution estimate of sea level changes throughout the Middle Miocene Climate Transition [*Kominz et al.*, 2008]. For the purposes of this discussion we multiply the eustatic sea level estimates of *Kominz et al.* [2008] by 1.48 to obtain "Apparent Sea Level" [*Pekar et al.*, 2002]. The timing, direction and amplitude of all bar one of the higher resolution (<1 m.y.) sea level trends are in good agreement with our independently derived estimates of the oxygen isotopic composition of seawater (δ^{18}Osw) (Figure 4c). For example, a maximum in the δ^{18}Osw record at ~16.2 Ma corresponds to a lowstand in the sea level record. δ^{18}Osw subsequently decreases between 16.2 and 16.0 Ma, while sea level rises.

δ^{18}Osw again increases between ~16.0 and 15.2 Ma while sea level falls between 15.6 Ma and 15.2 Ma, (suggesting an error in the age model of the sea level record). Between 15.2 and 14.8 Ma, δ^{18}Osw decreased by ~0.5‰, while Apparent Sea Level rose by ~50 m. The interval immediately following this major deglaciation interval of the Miocene Climatic Optimum represents the largest disagreement between the δ^{18}Osw and sea level records. Between 14.8 and 13.6 Ma our δ^{18}Osw record increased by ~0.8‰, implying a major glaciation, yet the sea level record shows no overall change over the same time interval. After 13.6 Ma, the δ^{18}Osw and sea level records again imply a more consistent history of ice volume change (Figure 4c). The increase in δ^{18}Osw between 14.8 and 13.6 is primarily driven by the well-documented global Middle Miocene increase in the benthic oxygen isotope record, and is widely interpreted as reflecting an increase in continental ice volume. Furthermore, an overall sea level lowering across the climate transition is obtained using backstripping techniques on the Marion Plateau [*John et al.*, 2004]. Therefore, this brief yet significant discrepancy between our δ^{18}Osw record and the sequence stratigraphic sea level record (between 14.8 and 13.6 Ma) suggests that the New Jersey/Delaware core holes do not capture the entire sea level history across the Middle Miocene climate transition, possibly due to progressive loss of marine strata during the Middle Miocene (K. G. Miller, personal communication, 2010). There are also both long-term and short-term discrepancies between different sequence stratigraphic sea level records. For example, the New Jersey records of *Kominz et al.* [2008] and *Miller et al.* [2005] suggest Middle Miocene sea level variations on the order of around 60 m, whereas the record of *Haq et al.* [1987] suggests Middle Miocene sea level variations on the order of 150 m (see *Müller et al.* [2008] for discussion of the long-term trends in these records). Improved independent records of Miocene sea level variability are urgently required.

[20] Estimating an overall increase in ice volume across the climate transition is difficult because there is a pronounced deglaciation event immediately prior to the main glaciation episode. Therefore, our overall estimate of ice volume increase depends on the time interval specified (Figure 4c). For example, the difference in δ^{18}Osw between the peak deglaciation at ~14.8 Ma and the postglacial maxima at ~12.7 Ma is around 1‰. However, a more representative estimate of the overall increase in ice volume could be taken between 15.3 Ma (which corresponds to a plateau in the benthic oxygen isotope record within the Miocene Climatic Optimum) and 12.5 Ma. Across this time interval, benthic δ^{18}O increased by ~0.9‰, BWT cooled ~1°C, and δ^{18}Ow increased by ~0.6‰. Translating this value into an ice volume equivalent requires estimation of the isotopic composition of ancient ice sheets, which may have had heavier δ^{18}O in warmer climates. However, the Pleistocene calibration of 0.08–0.11‰ per 10 m sea level [*Fairbanks and Matthews*, 1978; *Adkins et al.*, 2002] seems to be a reasonable estimate for the Middle Miocene [*Langebroek et al.*, 2010]. By using this range on our Middle Miocene δ^{18}Ow increase we infer a 55–75 m sea level fall. Considering the uncertainties in the oxygen isotope record (±0.1‰) and BWTs (~1.1°C), the error in our sea level estimates is about ±30 m. Our result is
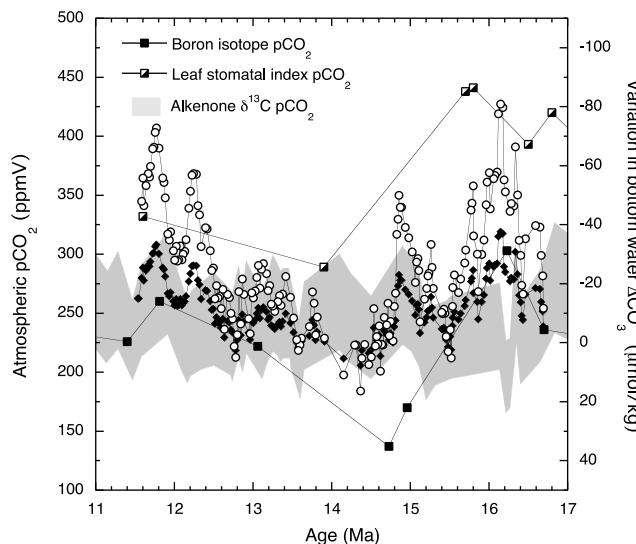
Figure 5. Estimated variations in bottom water saturation state at ODP Site 761B and atmospheric pCO_2 records reconstructed from leaf stomatal indices (hatched squares) [*Kürschner et al.*, 2008], boron isotopes (closed squares) [*Pearson and Palmer*, 2000], and alkenone $\delta^{13}C$ (gray shaded area) [*Pagani et al.*, 1999]. Bottom water saturation state variations were calculated using both the uncorrected (open circles) and corrected (closed diamonds) temperature records shown in Figure 4a, starting with an initial value of zero at 16.97 Ma, which is not shown (see text for details).

consistent with the 74.5 ± 29.5 m eustatic sea level fall across the climate transition determined by backstripping techniques on the Marion Plateau [*John et al.*, 2004].

4.2. Middle Miocene Saturation States

[21] A distinct advantage in using paired Mg/Ca and Li/Ca ratios to calculate temperatures is that it also allows variations in bottom water saturation state to be estimated (Figure 4d). The gray range in Figure 4c is assuming either a saturation state effect on the Mg/Ca record or not (section 4.1). Unfortunately we do not have a suitable %CaCO₃ or CCD record to compare to our record of estimated ΔCO_3^{2-}. The % coarse fraction of deep-sea sediment is controlled by many different factors, including the nature of overlying productivity, extent of winnowing, input of terrestrial clays, but also fragmentation of foraminiferal tests by corrosive bottom waters. If the latter process was the dominant control on % coarse fraction at Site 761, we would expect to see a positive correlation between % coarse fraction and our estimated ΔCO_3^{2-} variations. Some parts of our $\Delta CO_3 =$ record do appear to share some trends with the % coarse record, in particular between 16.6 and 16.0 Ma and between 14.0 and 11.5 Ma. However, in the interval between 16 and 14 Ma there is a possible antiphase relationship between the % coarse and ΔCO_3^{2-} records (Figure 4d). Perhaps unsurprisingly, it therefore appears that the major controls on the % coarse fraction of sediment at Site 761 changed between the Miocene Climatic Optimum and the climate transition.

[22] All else being equal, global bottom water saturation state is inversely proportional to atmospheric pCO_2. Although some changes in the total carbon inventory of the ocean-atmosphere system are to be expected across the MMCT, it is nevertheless interesting to compare our bottom water saturation state variations to Miocene records of atmospheric carbon dioxide (Figure 5). We start our saturation state calculations at 0 μmol/kg at 16.97 Ma (this initial arbitrary value is not shown) such that the records display only variations in saturation state rather than absolute values. In order to enable a first order comparison between these data, the axes in Figure 5 represent a scaling factor between pCO_2 and ΔCO_3^{2-} of 2.5. This is similar to the magnitude of the scaling expected between surface water (CO_3^{2-}) and atmospheric pCO_2, although this value is also dependent on several unknown factors including seawater total alkalinity and sea surface temperature. We also note that changes in bottom water saturation state may differ from changes in surface water (CO_3^{2-}), although we expect them to have similar trends. Our records of bottom water saturation state display a marked increase in the lead up to the major ice growth event of the middle Miocene, consistent with the decline in pCO_2 inferred from boron isotopes and fossil leaf stomatal index [*Pearson and Palmer*, 2000; *Kürschner et al.*, 2008] but apparently at odds with the relatively constant alkenone pCO_2 record [*Pagani et al.*, 1999] (Figure 5). This trend is matched by declining BWT (Figure 4). Following the glacial expansion, bottom water saturation state shows an overall decrease from around 13 Ma, again consistent with the increase in pCO_2 inferred from the boron isotope and fossil leaf stomatal index records. While there may be some uncertainties associated with applying modern calibrations to fossil leaves, the overall trend of the stomatal index data seems to be a robust indicator of relative changes in pCO_2. However, there is little change within the alkenone pCO_2 record through the Middle Miocene Climate Transition (Figure 5). It is therefore possible that the uncertainties associated with the alkenone proxy are relatively large compared to the CO_2 decrease. The cause of the Miocene changes in the ocean-atmosphere carbon system is unknown, but our records reaffirm the coupling between pCO_2 and global climate suggested by Quaternary climate records [*Petit et al.*, 1999]. Superimposed on these long-term trends are more rapid increases in bottom water saturation state associated with individual glaciation events (Figure 5). It is likely that these reflect sea level induced changes in shelf-basin carbonate deposition and alkalinity flux to the oceans, which may have led to additional transient decreases in atmospheric pCO_2 across the middle Miocene climate transition [*Merico et al.*, 2008]. The overall increase in bottom water saturation state across the climate transition is also consistent with the Middle Miocene shift in the Cenozoic barite calcium isotope record, which can be interpreted as reflecting an increased flux of Ca^{2+} (and hence alkalinity) to the oceans [*Griffith et al.*, 2008].

5. Conclusions

[23] Paired benthic foraminiferal Mg/Ca and Li/Ca records may be used together to reconstruct variations in BWT and saturation state (although absolute values of

these parameters depend on estimates of seawater Mg/Ca and Li/Ca). Bottom water temperatures cooled by ~1°C between 15.3 and 12.5 Ma, while the oxygen isotopic composition of seawater increased by ~0.6‰, although larger amplitude variations in $\delta^{18}Ow$ are observed between Miocene glacial maxima and minima. Our saturation state reconstructions support suggestions that the middle Miocene expansion of the Antarctic ice sheet was caused by declining pCO_2. We suggest that although the stepped decreases in sea level caused further episodic decreases in pCO_2 throughout the climate transition, background levels of pCO_2 began to recover following the main ice growth event, and bottom water temperatures warmed accordingly. Reconstructed ice volume appears relatively stable during this subsequent warming, suggesting that the ice sheet had grown large enough to be self-stabilizing to some extent (the hysteresis effect [*Pollard and DeConto*, 2005]). A similar pattern of CO_2 rebound is observed immediately after the earliest Oligocene ice growth event [*Pearson et al.*, 2009] and perhaps points to a shared negative feedback process associated with major glaciation events. Examples of potential negative feedback processes include oxidation of terrestrial/shelf organic matter caused by the sea level fall, or a temporary reduction in global silicate weathering rates [*Pagani et al.*, 1999; *Lear et al.*, 2004].

References

Adkins, J. F., K. McIntyre, and D. P. Schrag (2002), The salinity, temperature, and $\delta^{18}O$ of the glacial deep ocean, *Science*, *298*, 1769–1773, doi:10.1126/science.1076252.

Billups, K., and D. P. Schrag (2002), Paleotemperatures and ice volume of the past 27 Myr revisited with paired Mg/Ca and $^{18}O/^{16}O$ measurements on benthic foraminifera, *Paleoceanography*, *17*(1), 1003, doi:10.1029/2000PA000567.

Billups, K., and D. P. Schrag (2003), Application of benthic foraminiferal Mg/Ca ratios to questions of Cenozoic climate change, *Earth Planet. Sci. Lett.*, *209*, 181–195, doi:10.1016/S0012-821X(03)00067-0.

Boyle, E. A., and L. D. Keigwin (1985), Comparison of Atlantic and Pacific paleochemical records for the last 250,000 years: Changes in deep ocean circulation and chemical inventories, *Earth Planet. Sci. Lett.*, *76*, 135–150, doi:10.1016/0012-821X(85)90154-2.

Broecker, W. S., and T.-H. Peng (1982), *Tracers in the Sea*, Eldigo, Palisades, N. Y.

Bryan, S. P., and T. M. Marchitto (2008), Mg/Ca–temperature proxy in benthic foraminifera: New calibrations from the Florida Straits and a hypothesis regarding Mg/Li, *Paleoceanography*, *23*, PA2220, doi:10.1029/2007PA001553.

Burton, K. W., and D. Vance (2000), Glacial-interglacial variations in the neodymium isotope composition of seawater in the Bay of Bengal recorded by planktonic foraminifera, *Earth Planet. Sci. Lett.*, *176*, 425–441, doi:10.1016/S0012-821X(00)00011-X.

Coxall, H. K., P. A. Wilson, H. Pälike, C. H. Lear, and J. Backman (2005), Rapid stepwise onset of Antarctic glaciation and deeper calcite compensation in the Pacific Ocean, *Nature*, *433*, 53–57, doi:10.1038/nature03135.

Curry, W. B., and T. M. Marchitto (2008), A secondary ionization mass spectrometry calibration of *Cibicidoides pachyderma* Mg/Ca with temperature, *Geochem. Geophys. Geosyst.*, *9*, Q04009, doi:10.1029/2007GC001620.

DeConto, R. M., D. Pollard, P. A. Wilson, H. Pälike, C. H. Lear, and M. Pagani (2008), Thresholds for Cenozoic bipolar glaciation, *Nature*, *455*, 652–656, doi:10.1038/nature07337.

Elderfield, H., P. Yu, P. Anand, T. Kiefer, and B. Nyland (2006), Calibrations for benthic foraminiferal Mg/Ca paleothermometry and the carbonate ion hypothesis, *Earth Planet. Sci. Lett.*, *250*, 633–649, doi:10.1016/j.epsl.2006.07.041.

Fairbanks, R. G., and R. K. Matthews (1978), The marine oxygen isotope record in Pleistocene coral, Barbados, West Indies, *Quat. Res.*, *10*, 181–196, doi:10.1016/0033-5894(78)90100-X.

Flower, B. P., and J. P. Kennett (1993), Relations between Monterey Formation deposition and middle Miocene global cooling: Naples Beach section, Calif., *Geology*, *21*, 877–880, doi:10.1130/0091-7613(1993)021<0877:RBMFDA>2.3.CO;2.

Flower, B. P., and J. P. Kennett (1994), The middle Miocene climatic transition: East Antarctic ice sheet development, deep ocean circulation and global carbon cycling, *Palaeogeogr. Palaeoclimatol. Palaeoecol.*, *108*, 537–555, doi:10.1016/0031-0182(94)90251-8.

Griffith, E., A. Paytan, K. Caldeira, T. D. Bullen, and E. Thomas (2008), A dynamic marine calcium cycle during the past 28 million years, *Science*, *322*, 1671–1674, doi:10.1126/science.1163614.

Hall, J. M., and L. H. Chan (2004), Li/Ca in multiple species of benthic and planktonic foraminifera: Thermocline, latitudinal, and glacial-interglacial variation, *Geochim. Cosmochim. Acta*, *68*, 529–545, doi:10.1016/S0016-7037(03)00451-4.

Haq, B. U., J. Hardenbol, and P. R. Vail (1987), Chronology of fluctuating sea levels since the Triassic, *Science*, *235*, 1156–1167, doi:10.1126/science.235.4793.1156.

Healey, S. L., R. C. Thunell, and B. H. Corliss (2008), The Mg/Ca-temperature relationship of benthic foraminiferal calcite: New core-top calibrations in the <4°C temperature range, *Earth Planet. Sci. Lett.*, *272*, 523–530, doi:10.1016/j.epsl.2008.05.023.

Holbourn, A., W. Kuhnt, J. A. Simo, and Q. Li (2004), Middle Miocene isotope stratigraphy and paleoceanographic evolution of the northwest and southwest Australian margins (Wombat Plateau and Great Australian Bight), *Palaeogeogr. Palaeoclimatol. Palaeoecol.*, *208*, 1–22, doi:10.1016/j.palaeo.2004.02.003.

Hsü, K. J., J. McKenzie, H. Oberhänsli, and R. C. Wright (1984), South Atlantic Cenozoic paleoceanography, *Initial Rep. Deep Sea Drill. Proj.*, *73*, 771–785.

John, C. M., G. D. Karner, and M. Mutti (2004), $\delta^{18}O$ and Marion Plateau backstripping: Combining two approaches to constrain late middle Miocene eustatic amplitude, *Geology*, *32*, 829–832, doi:10.1130/G20580.1.

Jordan, K. A. (2008), Evaluating carbonate saturation effects on magnesium calcium core top calibration in benthic foraminifera, M.Sc. thesis, Rutgers, State Univ. of N. J., New Brunswick, N. J.

Katz, M. E., K. G. Miller, J. D. Wright, B. S. Wade, J. V. Browning, B. S. Cramer, and Y. Rosenthal (2008), Stepwise transition from the Eocene greenhouse to the Oligocene icehouse, *Nat. Geosci.*, *1*, 329–334, doi:10.1038/ngeo179.

Kominz, M. A., J. V. Browning, K. G. Miller, P. J. Sugarman, S. Mizintseva, and C. R. Scotese (2008), Late Cretaceous to Miocene sea-level estimates from the New Jersey and Delaware coastal plain coreholes: An error analysis, *Basin Res.*, *20*, 211–226, doi:10.1111/j.1365-2117.2008.00354.x.

Kürschner, W. M., Z. Kvacek, and D. L. Dilcher (2008), The impact of Miocene atmospheric carbon dioxide fluctuations on climate and the evolution of terrestrial ecosystems, *Proc. Natl. Acad. Sci. U. S. A.*, *105*, 449–453, doi:10.1073/pnas.0708588105.

Langebroek, P. M., A. Paul, and M. Schulz (2010), Simulating the sea level imprint on marine oxygen isotope records during the middle Miocene using an ice sheet–climate model, *Paleoceanography*, *25*, PA4203, doi:10.1029/2008PA001704.

Lear, C. H., and Y. Rosenthal (2006), Benthic foraminiferal Li/Ca: Insights into Cenozoic seawater carbonate saturation state, *Geology*, *34*, 985–988, doi:10.1130/G22792A.1.

Lear, C. H., H. Elderfield, and P. A. Wilson (2000), Cenozoic deep-sea temperatures and global ice volumes from Mg/Ca in benthic foraminiferal calcite, *Science*, *287*, 269–272, doi:10.1126/science.287.5451.269.

Lear, C. H., Y. Rosenthal, and N. Slowey (2002), Benthic foraminiferal Mg/Ca-paleothermometry: A revised core-top calibration, *Geochim. Cosmochim. Acta*, *66*, 3375–3387, doi:10.1016/S0016-7037(02)00941-9.

Lear, C. H., Y. Rosenthal, H. K. Coxall, and P. A. Wilson (2004), Late Eocene to early Miocene ice sheet dynamics and the global carbon cycle, *Paleoceanography*, *19*, PA4015, doi:10.1029/2004PA001039.

Lear, C. H., T. R. Bailey, P. N. Pearson, H. K. Coxall, and Y. Rosenthal (2008), Cooling and ice growth across the Eocene-Oligocene transition, *Geology*, *36*, 251–254, doi:10.1130/G24584A.1.

Marchitto, T. M., S. P. Bryan, W. B. Curry, and D. C. McCorkle (2007), Mg/Ca temperature calibration for the benthic foraminifer *Cibicidoides pachyderma*, *Paleoceanography*, *22*, PA1203, doi:10.1029/2006PA001287.

Marriott, C. S., G. M. Henderson, R. Crompton, M. Staubwasser, and S. Shaw (2004), Effect of mineralogy, salinity, and temperature on Li/Ca and Li isotope composition of calcium carbonate, *Chem. Geol.*, *212*, 5–15, doi:10.1016/j.chemgeo.2004.08.002.

Martin, P. A., D. W. Lea, Y. Rosenthal, N. J. Shackleton, M. Sarnthein, and T. Papenfuss (2002), Quaternary deep sea temperature histories derived from benthic foraminiferal Mg/Ca, *Earth Planet. Sci. Lett.*, *198*, 193–209, doi:10.1016/S0012-821X(02)00472-7.

Mawbey, E. M., C. H. Lear, and H. K. Coxall (2009), Trace metal proxy records across the Eocene/Oligocene boundary from ODP Leg 199, abstract presented at First Antarctic Climate Evolution Meeting, Minist. de Cienc. e Innovación, Gob. de España, Granada, Spain.

Merico, A., T. Tyrrell, and P. A. Wilson (2008), Eocene/Oligocene ocean de-acidification linked to Antarctic glaciation by sea-level fall, *Nature*, *452*, 979–982, doi:10.1038/nature06853.

Miller, K. G., R. G. Fairbanks, and G. S. Mountain (1987), Tertiary oxygen isotope synthesis, sea level history, and continental margin erosion, *Paleoceanography*, *2*, 1–19, doi:10.1029/PA002i001p00001.

Miller, K. G., M. A. Kominz, J. V. Browning, J. D. Wright, G. S. Mountain, M. E. Katz, P. J. Sugarman, B. S. Cramer, N. Christie-Blick, and S. F. Pekar (2005), The Phanerozoic record of global sea-level change, *Science*, *310*, 1293–1298, doi:10.1126/science.1116412.

Müller, R. D., M. Sdolias, C. Gaina, B. Steinberger, and C. Heine (2008), Long-term sea-level fluctuations driven by ocean basin dynamics, *Science*, *319*, 1357–1362, doi:10.1126/science.1151540.

Pagani, M., M. A. Arthur, and K. H. Freeman (1999), Miocene evolution of atmospheric carbon dioxide, *Paleoceanography*, *14*, 273–292, doi:10.1029/1999PA900006.

Pagani, M., K. Caldeira, R. Berner, and D. J. Beerling (2009), The role of terrestrial plants in limiting atmospheric CO_2 decline over the past 24 million years, *Nature*, *460*, 85–88, doi:10.1038/nature08133.

Pearson, P. N., and M. R. Palmer (2000), Atmospheric carbon dioxide concentrations over the past 60 million years, *Nature*, *406*, 695–699, doi:10.1038/35021000.

Pearson, P. N., G. L. Foster, and B. S. Wade (2009), Atmospheric carbon dioxide through the Eocene-Oligocene climate transition, *Nature*, *461*, 1110–1113, doi:10.1038/nature08447.

Pekar, S. F., N. Christie-Blick, M. A. Kominz, and K. G. Miller (2002), Calibration between eustatic estimates from backstripping and oxygen isotopic records for the Oligocene, *Geology*, *30*, 903–906, doi:10.1130/0091-7613(2002)030<0903:CBEEFB>2.0.CO;2.

Petit, J. R., et al. (1999), Climate and atmospheric history of the past 420,000 years from the Vostok ice core, Antarctica, *Nature*, *399*, 429–436, doi:10.1038/20859.

Pollard, D., and R. M. DeConto (2005), Hysteresis in Cenozoic Antarctic ice-sheet variations, *Global Planet. Change*, *45*, 9–21, doi:10.1016/j.gloplacha.2004.09.011.

Rea, D. K., and M. W. Lyle (2005), Paleogene calcite compensation depth in the eastern subtropical Pacific: Answers and questions, *Paleoceanography*, *20*, PA1012, doi:10.1029/2004PA001064.

Rosenthal, Y., C. H. Lear, D. W. Oppo, and B. K. Linsley (2006), Temperature and carbonate ion effects on Mg/Ca and Sr/Ca ratios in benthic foraminifera: Aragonitic species *Hoeglundina elegans*, *Paleoceanography*, *21*, PA1007, doi:10.1029/2005PA001158.

Sabine, C., R. Feely, N. Gruber, R. M. Key, K. Lee, J. L. Bullister, R. Wanninkhof, C. S. Wong, D. W. R. Wallace, and B. Tilbrook (2004), The oceanic sink for anthropogenic CO_2, *Science*, *305*, 367–371, doi:10.1126/science.1097403.

Shackleton, N. J. (1974), Attainment of isotopic equilibrium between ocean water and the benthonic foraminifera genus *Uvigerina*: Isotopic changes in the ocean during the last glacial, *Colloq. Int. CNRS*, *219*, 203–209.

Shackleton, N. J., and J. P. Kennett (1975), Paleotemperature history of the Cenozoic and the initiation of Antarctic glaciation: Oxygen and carbon isotope analyses in DSDP Sites 277, 279, and 281, *Initial Rep. Deep Sea Drill. Proj.*, *29*, 743–755.

Shevenell, A. E., J. P. Kennett, and D. W. Lea (2008), Middle Miocene ice sheet dynamics, deep-sea temperatures, and carbon cycling: A Southern Ocean perspective, *Geochem. Geophys. Geosyst.*, *9*, Q02006, doi:10.1029/2007GC001736.

Sosdian, S., and Y. Rosenthal (2009), Deep-sea temperature and ice volume changes across the Pliocene-Pleistocene climate transitions, *Science*, *325*, 306–310, doi:10.1126/science.1169938.

Stoffynegli, P., and F. T. MacKenzie (1984), Mass balance of dissolved lithium in the oceans, *Geochim. Cosmochim. Acta*, *48*, 859–872, doi:10.1016/0016-7037(84)90107-8.

Vincent, E., and W. H. Berger (1985), Carbon dioxide and polar cooling in the Miocene: The Monterey hypothesis, in *The Carbon Cycle and Atmospheric CO_2: Natural Variations Archean to Present*, *Geophys. Monogr. Ser.*, vol. 32, edited by E. T. Sundquist and W. S. Broecker, pp. 455–468, AGU, Washington, D. C.

Yu, J., and H. Elderfield (2008), Mg/Ca in the benthic foraminifera *Cibicidoides wuellerstorfi* and *Cibicidoides mundulus*: Temperature versus carbonate ion saturation, *Earth Planet. Sci. Lett.*, *276*, 129–139, doi:10.1016/j.epsl.2008.09.015.

Zachos, J., M. Pagani, L. Sloan, E. Thomas, and K. Billups (2001), Trends, rhythms, and Aberrations in global climate 65 Ma to Present, *Science*, *292*, 686–693, doi:10.1126/science.1059412.

C. H. Lear and E. M. Mawbey, School of Earth and Ocean Sciences, Cardiff University, Main Building, Park Place, Cardiff CF10 3YE, UK. (learc@cf.ac.uk; mawbeyem@cf.ac.uk)

Y. Rosenthal, Institute of Marine and Coastal Sciences and Department of Geological Sciences, Rutgers, State University of New Jersey, 71 Dudley Rd., New Brunswick, NJ 08901, USA.